HHS Public Access

Author manuscript

*Behav Brain Res*. Author manuscript; available in PMC 2018 August 30.

Published in final edited form as:

*Behav Brain Res*. 2017 August 30; 333: 161–170. doi:10.1016/j.bbr.2017.06.045.

# Operant responding for optogenetic excitation of LDTg inputs to the VTA requires D1 and D2 dopamine receptor activation in the NAcc

**Stephan Steidl**[a,*], **Shannon O'Sullivan**[a], **Dustin Pilat**[a], **Nancy Bubula**[b], **Jason Brown**[b], and **Paul Vezina**[b]

[a]Department of Psychology, Loyola University Chicago, 1032 West Sheridan Road, Chicago, IL 60626, United States

[b]Department of Psychiatry and Behavioral Neuroscience, University of Chicago, 5481 South Maryland Avenue, Chicago, IL 60637, United States

## Abstract

Behavioral studies in rats and mice indicate that laterodorsal tegmental nucleus (LDTg) inputs to the ventral tegmental area (VTA) importantly contribute to reward function. Further evidence from anesthetized rat and mouse preparations suggests that these LTDg inputs may exert this effect by regulating mesolimbic dopamine (DA) signaling. Direct evidence supporting this possibility remains lacking however. To address this lack, rat LDTg neurons were transfected with adeno-associated viral vectors encoding channelrhodopsin2 and eYFP (ChR2) or eYFP alone (eYFP) and rats were subsequently trained to lever press for intracranial self-stimulation (ICSS) of the inputs of these neurons to the VTA. First, we found that DA overflow in the forebrain nucleus accumbens (NAcc) increased maximally during ICSS to approximately 240% of baseline levels in ChR2, but not in eYFP, rats. Based on these findings, we next tested the contribution of NAcc D1 and D2 DA receptors to the reinforcing effects of optogenetic excitation of LDTg inputs to the VTA. Microinjecting SCH23390 or raclopride, D1 and D2 DA receptor antagonists respectively, into the NAcc significantly reduced operant responding for this stimulation. Together these results demonstrate for the first time that optogenetic ICSS of LDTg inputs to the VTA increases DA overflow in the NAcc and requires activation of D1 and D2 DA receptors in this site.

### Keywords

pedunculopontine tegmental nucleus; reward; mesopontine; microdialysis; raclopride; SCH 23390

[*]Corresponding Author: Department of Psychology, Loyola University Chicago, 1032 West Sheridan Road, Chicago, Illinois, 60626 USA. Tel: 773-508-2971; Fax: 773-508-8713; ssteidl@luc.edu.

## 1. Introduction

Dopamine (DA) neuron activity and forebrain DA levels are correlated with reinforcement, reward prediction and can signal saliency and aversion [1–5]. The ventral tegmental area (VTA) receives afferents from several brain areas [6,7], some of which can regulate the firing activity of VTA DA neurons [8, 9]. Different afferents may convey select types of information to the VTA that are important for different aspects of motivated behavior. The laterodorsal tegmental nucleus (LDTg; also referred to as LDT by others) provides one source of afferent input to the ventral tegmental area [VTA; 6, 7, 10, 11] and specifically to DA neurons in this site [6]. Recent studies show that optogenetic excitation of LDTg inputs to the VTA is rewarding in rats [12, 13] and in mice [14, 15].

In rats, approximately 50% of LDTg inputs to the VTA form asymmetric excitatory synapses that preferentially give rise to mesoaccumbens projections terminating in the nucleus accumbens (NAcc) core and medial shell [16]. Electrical stimulation of the LDTg in anesthetized rats has been shown to increase DA efflux in the NAcc core [17] but the effects of operant responding for optogenetic excitation of LDTg inputs to the VTA on DA overflow in this site remain unknown. The core subregion of the NAcc contributes importantly to the expression of motivated behaviors (e.g., [18, 19]). Thus, the reinforcing effects of optogenetic intracranial self-stimulation (ICSS) of LDTg inputs to the VTA in rats could involve DA signaling in this site. To address this possibility, we used 1) microdialysis to measure NAcc DA overflow before, during, and after optogenetic ICSS of LDTg inputs to the VTA, and 2) microinjections of D1 (SCH 23390) or D2 (Raclopride) DA receptor antagonists into the NAcc core or shell prior to ICSS.

## 2. Materials and Methods

### 2.1. Subjects

Thirty-three adult male Long-Evans rats bred at Loyola University Chicago were housed in a colony room on a 12h:12h light:dark cycle (lights off at 9 am) with food and water available ad libitum. Rats were group-housed after weaning but were individually housed following surgery for the remainder of the experiment. All experiments were conducted in accordance with the National Institutes of Health Guide for the Care and Use of Laboratory Animals and with approval of the Loyola University Chicago Animal Care and Use Committee.

### 2.2. Stereotaxic injections of recombinant adeno-associated virus and probe implantation

Each rat (~ 300 grams at the time of surgery) was anesthetized with a combination of ketamine and xylazine (57 mg/kg and 9 mg/kg i.p., respectively) and secured in a stereotaxic apparatus. Isoflurane (2–3% in 1 L/min Oxygen) was introduced after approximately 40 minutes to maintain surgical anesthesia for the duration of surgery. Adeno-associated viral vectors (~ $10^{12}$ infectious units/ml, serotype 5) were obtained from the University of North Carolina vector core facility. Rats were bilaterally infused with AAV into the LDTg to express either channelrhodopsin-2 fused to eYFP (AAV-CaMKIIα-ChR2(H134R)-eYFP; n = 25, referred to as ChR2 rats) or only eYFP (AAV-CamKIIα-eYFP; n = 8, referred to as eYFP rats). Both vectors were under the control of the CamKIIα promotor. In all cases AAV

infusions were made using a 10μl syringe controlled by an automated infusion pump (UMP 3; World Precision Instruments) attached to one of the stereotaxic manipulator arms. The injector needle was lowered into each LDTg from the front along an angled trajectory of 30° from the vertical. Three injections (200 nl per injection; 100nl/min) per hemisphere were made at the following coordinates relative to Bregma according to the rat brain atlas of Paxinos & Watson [20]: (1) A-P −8.7, M-L ± 1.13, D-V −7.0, (2) A-P −8.5, M-L ± 1.13, D-V −6.8, (3) A-P −8.3, M-L ± 1.13, D-V −6.4. The needle tip was lowered to the most caudal site for the first injection, retracted to the second site for the second injection, and retracted to the third site for the third injection. Following each infusion, the injector was left in place for five minutes to allow for diffusion of virus particles from the needle tip. Following removal of the syringe needle, all rats were bilaterally implanted with 200 μm optical fibers, threaded through 2.5 mm stainless steel ferrules, and aimed at the dorsal border of the VTA (AP −6.0, ML ±0.5, DV −8.0 from bregma and angled laterally at 10° from the vertical). For the microdialysis experiment eighteen rats (10 ChR2 and 8 eYFP) were also unilaterally implanted with guide cannulae (CMA11; Harvard Apparatus) aimed at the nucleus accumbens core (AP +2.0, ML ±1.2, DV −7.6 from bregma and angled laterally at 10° from the vertical). For the DA receptor antagonist experiments, six of the remaining ChR2 rats were also bilaterally implanted with guide cannulae (22 ga, Plastics One Inc.) aimed at the NAcc core (AP +1.7, ML ±1.6, DV −7.3 from bregma and angled laterally at 10° from the vertical), while the remaining 9 ChR2 rats were also bilaterally implanted with guide cannulae aimed at the NAcc shell to provide additional data for this NAcc subnucleus (see Table 1). The shell cannulae were inserted from the opposite hemisphere through the midline, and angled laterally at 20° from vertical [21]. In order to avoid collision of the bilateral cannulae into the shell, two different sets of coordinates were used: (1) AP +1.7, ML ±1.0, DV −7.6 from bregma, and (2) AP +1.2, ML ±1.8, DV −7.8 from bregma. These were counterbalanced between the left and right hemispheres across rats. Angled NAcc shell cannulae placements were used to minimize any contribution of drug solutions diffusing dorsally up the cannulae tracks [22] into the NAcc core. All implants were secured to the rat skull using a combination of stainless steel screws and dental cement. Immediately after surgery and again at 24 hr and 48 hr after surgery, each rat received a 5ml s.c. injection of sterile saline containing Ketoprofen (5 mg/kg) and Baytril (enrofloxacin, 10 mg/kg).

### 2.3. VTA Intracranial self-stimulation (ICSS) training

**2.3.1. Apparatus—**Operant conditioning chambers (25 × 27 × 30 cm; MedAssociates Inc.) were equipped with two retractable levers located on one wall of the chamber, a green house light, and a white cue light located above and between the two retractable levers, respectively. Optical tethers consisted of a diode-pumped solid state laser (473 nm, 150 mW; OEM Laser Systems or OptoEngine LLC) coupled to a 62.5 μm core, 0.22 NA standard multimode hard cladding optical fiber (Thor Labs) that passed through a single-channel optical rotary joint (Doric Lenses) prior to being split 50:50 with a fused optical coupler (Precision Fiber Products). Light intensity was set to 15–18 mW per split fiber.

**2.3.2. ICSS Training—**Training started eight weeks after surgery. Rats were connected to optical tethers immediately prior to each behavioral testing session. All rats underwent between 12 and 15 daily 30-min sessions during which pressing of one retractable lever (the

reinforced lever) resulted in 30 10 ms pulses of 473 nM light delivered at 20 Hz and illumination of the cue light for 3 seconds. No priming stimulation was given at any time and presses on the reinforced lever made within 3 seconds of the previous lever press were recorded but did not result in laser activation. Presses on the alternate retractable lever (the non-reinforced lever) were recorded but had no programmed consequence. Stimulation parameters chosen for ICSS training (i.e. pulse durations and pulse frequencies) were previously shown to be optimal, resulting in reliable and consistent lever-pressing rates [12].

### 2.4. *In vivo* microdialysis

**2.4.1. Procedure—**A few hours after the final ICSS training session, rats were slightly anesthetized with isoflurane and concentric microdialysis probes (CMA11, 2mm active membrane length protruding from the tip of the guide cannula; Harvard Apparatus) were lowered into the NAcc for microdialysis testing the following day. After probe insertion, rats were housed individually in 5 gal plastic buckets and kept in the same room as the ICSS testing apparatus overnight with food and water freely available. Rats were connected via a steel-spring tether to a liquid swivel and collection vial positioned outside the bucket. Probes were perfused with artificial cerebrospinal fluid at 0.3 μl/min overnight. The following morning the perfusion rate was increased to 1.5 μl/min and rats remained in the plastic bucket for an additional two hours after which each rat was transferred to the same operant chamber in which it previously received ICSS training. Both levers remained retracted and the house light and cue light remained off for the first thirty minutes. During this period three microdialysis samples were collected. A 30 min ICSS testing session subsequently ensued and an additional three microdialysis samples were collected. Finally rats remained in the operant chambers with the levers retracted and the house light turned off for one hour following the ICSS session and six additional microdialysis samples were collected. All samples were collected at 10 min intervals. Microdialysis probes were then removed and rats were returned to their home cages. All samples were immediately frozen on dry ice and stored at −80 °C for later assessment of DA levels.

**2.4.2 Chromatography—**HPLC-EC was conducted using a dual-piston Shimadzu LC-10AD pump set to 1.1ml/min, a 10 cm ODS-C18 3mm column (maintained at 35° C), an ESA Model 5100 Coulochem detector with a conditioning cell (oxidizing at +300mV) placed prior to a Model 5011 high sensitivity analytical cell (electrodes set to +50mV and −350mV), and a 0.04M sodium acetate mobile phase containing 0.3mM $Na_2$ EDTA, 0.5mM octyl sodium sulfate, 1% methanol, and 2.0% acetonitrile (pH 3.76). 15 μl dialysate samples were introduced into the mobile phase via a Rheodyne injection valve. Extracellular concentrations of DA were estimated from peak areas using Shimadzu CLASS-VP (Shimadzu Scientific Instruments, Columbia, MD) software.

### 2.5. NAcc microinjection of SCH23390 or Raclopride

**2.5.1. Drugs—**SCH23390 and raclopride were purchased from Sigma-Aldrich (St. Louis, MO) and were dissolved in sterile saline and bilaterally injected at a volume of 0.3 μl.

**2.5.2. Procedure—**Following completion of ICSS training, each rat in this experiment received a total of 4 additional testing sessions during which the effects of the D1 DA

receptor antagonist SCH 23390 (0 and 0.6 μg/0.3 μl) and the D2 DA receptor antagonist Raclopride (0 and 1 μg/0.3 μl) were tested. All rats were tested under each of the four conditions in a manner that counterbalanced antagonist and dose. Rats received an injection-free ICSS training day between the second and third tests. The doses of SCH 23390 and raclopride were chosen based on previous studies showing no significant effects on open-field locomotion at doses comparable to those used in the present experiments [23–25]. Rats administered the antagonists into the NAcc core and shell were tested identically.

For the antagonist microinjections, rats were gently restrained and bilateral injection cannulae (28 ga, Plastics One Inc.) were lowered to a depth 2 mm below the chronically implanted guide cannulae. Injection cannuale were connected to 2 μl Hamilton syringes via PE20 tubing. Injections were made using an automated infusion pump (Chemyx) at a rate of 0.2 μl/min. Injection cannulae were left in place for an additional 1 min before they were removed and the obturators were replaced. Rats were then connected to optic tethers and ICSS testing begun.

### 2.6. Histology

After completion of behavioral testing (approximately 10–11 weeks after AAV infusion) each rat was deeply anesthetized with chloral hydrate (300 mg/kg, i.p.) and was transcardially perfused with 0.1 M phosphate buffer (PB) followed by 4% (W/V) paraformaldehyde in 0.1 M PB, pH 7.3. The brains were removed and left in 4% paraformaldehyde for 2 hours at 4°C and then transferred to an 18% sucrose solution in PB overnight. Coronal cryosections (40 μm) throughout the extent of the LDTg and VTA were prepared for each rat. Free-floating LDTg sections were processed for double fluorescence immunohistochemistry to detect choline acetyl transferase (ChAT; 1:100 goat anti-ChAT primary antibody; AB144P, EMD Millipore) and GFP/YFP (1:1500 mouse anti-GFP/YFP primary antibody; A11120, Life Technologies) in the same tissue. Tissues were subsequently incubated with donkey anti-goat secondary antibody conjugated to AlexaFluor594 (1:500; A11058, Life Technologies) and rabbit anti-mouse secondary antibody conjugated to AlexaFluor488 (1:500; A21204, Life Technologies). Sections were mounted onto gelatin-coated slides and coverslipped with Fluormount (Electron Microscopy Sciences) and viewed using confocal fluorescence microscopy.

The boundaries of eYFP expression relative to the boundaries of the LDTg observed in the rostral, medial, and caudal portions of the LDTg were summarized on three LDTg sections for each rat (Bregma – 8.52; – 8.76, – 9.00, respectively). Some sections containing the VTA were not used for fluorescence immunohistochemistry but rather mounted onto gelatin-coated slides, stained with cresyl violet, and coverslipped with Permount (Electron Microscopy Sciences). These sections were used to determine optic probe locations using a standard light microscope.

Coronal cryosections (40 μm) throughout the extent of the NAcc were mounted onto gelatin-coated slides, stained with cresyl violet, and coverslipped with Permount. These sections were used to determine injection cannulae and microdialysis probe locations using a standard light microscope.

### 2.7. Statistical analyses

Final statistical analysis was based on 12 rats in the microdialysis experiment (n = 6 ChR2 and 6 eYFP), 6 ChR2 rats in the NAcc core microinjection experiment and 7 ChR2 rats in the NAcc shell microinjection experiment (see Table 1). Six ChR2 and 2 eYFP were not included, either because eYFP expression was detected outside the bounds of the LDTg or because cannulae placements were outside the NAcc. Otherwise, optic fiber tips were determined to be either within or immediately dorsal to the VTA (Fig 2B), microdialysis probe placements were within the NAcc (Fig 3C and 3D), and injection cannulae tip placements were within the NAcc core (Fig 4E) or shell (Fig 5E).

Lever pressing data were analyzed using either between-within or fully within repeated-measures ANOVA. Degrees of freedom were adjusted with the Greenhouse–Geisser method when the sphericity assumption was violated. Significant effects were further analyzed using Tukey's HSD post-hoc test. The latencies to the first reinforced lever press in the various pharmacological treatment conditions were analyzed using within-subjects t-tests. Maximal % baseline increases in NAcc DA overflow during ICCS in ChR2 and eYFP rats were compared using a between-subjects t-test, while the time course of NAcc DA overflow was analyzed using a between-within subjects ANOVA followed by post-hoc comparisons with Tukey's HSD test.

## 3. Results

### 3.1. Detection of eYFP in LDTg cells and their inputs to the VTA

We used ChAT immunofluorescence to outline the anatomical boundaries of the LDTg (Fig 1B). Following LDTg transfection with CAMKII-ChR2-eYFP (Fig 1A) we observed eYFP immunofluorescence within the boundaries of the LDTg (Fig 1B′). Some eYFP expression was also observed immediately outside the boundaries of the LDTg (Fig 1B′, 1E, 1F, 1G) but eYFP-labeled cell bodies were not observed in the adjacent PPTg. In the PPTg, however, eYFP-expressing processes were observed, some in the vicinity of ChAT-labeled cells (Fig 1D, 1D′, 1D″). Within the LDTg, eYFP expression was observed in both cholinergic and non-cholinergic LDTg cells (Figures 1C, 1C, 1C″). In VTA sections eYFP immunofluorescence was used to evaluate VTA innervation by transfected LDTg cells. Within the VTA, we detected fibers expressing eYFP in the proximity of optic probes (Fig 1H, 1I, 1I′, 1I″).

### 3.2. Optogenetic excitation of LDTg inputs to the VTA reinforces lever-pressing in rats

All ChR2 rats tested learned to lever press for VTA light stimulation, pressing the reinforced lever significantly more than the non-reinforced lever starting on the second training day. eYFP rats pressed either lever at equally low numbers throughout the training period (Fig 2A). ANOVA revealed a significant main effect of GROUP [$F_{1,23} = 35.58$, $p<0.001$] and a GROUP × SESSION × LEVER interaction [$F_{4.03, 92.63} = 5.03$, $p<0.01$]. Tukey post-hoc comparisons confirmed that ChR2 rats pressed the reinforced lever significantly more than the non-reinforced lever during training sessions 2 through 12 [p's<0.001].

### 3.3. Operant responding for optogenetic excitation of LDTg inputs to the VTA increases NAcc DA overflow

The day after completion of training, 6 ChR2 and 6 eYFP rats were tested for NAcc DA overflow before, during, and after optogenetic VTA ICSS of LDTg inputs. While baseline levels of DA did not differ between the two groups, lever pressing for optogenetic excitation of LDTg inputs to the VTA resulted in significant increases in NAcc DA overflow relative to baseline in ChR2, but not in eYFP, rats. After the 30min VTA ICSS session and retraction of the levers, NAcc DA overflow declined back to baseline levels over the subsequent hour (Fig 3A). ANOVA revealed a significant main effect of GROUP [$F_{1,10} = 9.12$, $p<0.05$] and a significant GROUP × TIME interaction [$F_{1,110} = 2.99$, $p<0.01$]. Tukey post-hoc comparisons showed that NAcc DA overflow was significantly elevated in ChR2 compared to eYFP rats throughout the ICSS session (30–60 min; p's<0.05–0.01) and in the first time bin following termination of the ICSS session (70 min; $p<0.01$). While DA overflow in ChR2 rats showed fluctuations during ICSS, the levels of overflow observed did not differ significantly from one another during this period. In eYFP control rats, that did not lever press during the ICSS session (Fig 3C), NAcc DA overflow fluctuated around baseline levels throughout the experiment (Fig 3A). The average maximal increase in NAcc DA overflow during the ICSS session in ChR2 rats (approximately 240% of baseline levels) was significantly greater than in eYFP rats (Fig 3B [$t_{10} = 3.23$, $p<0.01$]). Maximal overflow for each rat was taken as the highest DA peak achieved during the ICSS period. Notably, the significant increase in maximal NAcc DA overflow during ICSS in ChR2 relative to eYFP rats (Fig 3B) paralleled the significant difference between these two groups in presses on the reinforced lever (Fig 3C; GROUP × LEVER interaction [$F_{1,10} = 47.48$, $p<0.001$]; Tukey post-hoc comparisons showed that ChR2 rats pressed the reinforced lever significantly more than eYFP rats [$p<0.01$]).

### 3.4. Operant responding for optogenetic excitation of LDTg inputs to the VTA is dependent on activation of NAcc core and shell D1 and D2 DA receptors

Given that VTA ICSS of LDTg inputs increased NAcc core DA overflow we next tested the contributions of D1 or D2 DA receptors in this site to the reinforcing effects of VTA ICSS of LDTg inputs. Relative to saline, infusions of either SCH23390 or raclopride into the NAcc core significantly reduced the total number of reinforced lever presses for optogenetic VTA ICSS of LDTg inputs in ChR2 rats (Fig 4A and 4B). Presses on the non-reinforced lever were not affected. In each case, the ANOVA revealed a significant ANTAGONIST × LEVER interaction [$F_{1,5} = 9.43$ for SCH23390 and 9.83 for raclopride, p's<0.05] and Tukey post-hoc comparisons confirmed significant reductions in reinforced lever pressing following either receptor antagonist (p's<0.05). Time course analyses revealed a gradual manifestation of these effects with significant reductions in reinforced lever pressing appearing 11 and 6 minutes following infusion into the NAcc core of SCH23390 and raclopride, respectively (Fig 4C and 4D). The ANOVA found significant ANTAGONIST × TIME interactions in each case [$F_{29,145} = 4.14$ for SCH23390 and 4.33 for raclopride, p's<0.001] with Tukey post-hoc comparisons showing significant reductions (p's<0.05–0.01) from 11 (SCH23390) and 6 minutes (Raclopride) through the remainder of the ICSS test session. Latencies to the first reinforced lever press were not significantly affected by either receptor antagonist.

LDTg inputs to the VTA also synapse on DA neurons that project to the NAcc medial shell [16]. As a recent report indicated a role for D1 and D2 DA receptors in the lateral shell of the NAcc in the acquisition of Pavlovian conditioned place preference for optogenetic excitation of LDTg inputs to the VTA in mice [15], we repeated the above experiment in the medial NAcc shell to further assess the contribution of DA receptors in this NAcc subnucleus. Practically identical effects were observed following microinjection of either SCH23390 or raclopride into the NAcc shell. In each case the total numbers of reinforced, but not non-reinforced, lever presses for optogenetic VTA ICSS of LDTg inputs were significantly reduced (Fig 5A and Fig 5B). The ANOVA showed significant ANTAGONIST × LEVER interactions [$F_{1,6}$ = 30.58 for SCH23390 and 10.86 for raclopride, p's<0.05], and the time course analyses showed significant reductions (p's<0.05–0.01) in reinforced lever pressing beginning 9 and 10 minutes following NAcc shell SCH23390 (Fig 5C) or raclopride (Fig 5D) infusions, respectively. The ANOVA showed significant ANTAGONIST × TIME interactions ($F_{29,174}$ = 17.09 for SCH23390 and 10.74 for raclopride, p<0.001). Again, latencies to the first reinforced lever press were not significantly affected by either receptor antagonist.

## 4. Discussion

The present findings show that optogenetic ICSS of LDTg inputs to the VTA in rats increases NAcc DA overflow and requires the stimulation of D1 and D2 DA receptors by this DA in this site. This confirms previous findings that experimenter-administered electrical stimulation of LDTg cell bodies increases NAcc DA efflux in anaesthetized rats [17] and importantly extends them to show that its stimulation of NAcc forebrain DA receptors is necessary for VTA ICSS of LDTg inputs. Thus, the reinforcing effects of optogenetic excitation of LDTg inputs to the VTA in rats involve activation of mesolimbic DA projections to the NAcc and depend on both D1 and D2 DA receptor activation in this site.

The boundaries of the LDTg are traditionally defined by the distribution of cholinergic neurons [26, 27]. Accordingly, we used ChAT-labeling to identify these boundaries. The viral construct used in the current studies is not selective for neuronal phenotypes and we consequently observed, within the areas outlined by ChAT-labeling, eYFP-labeled cells and eYFP/ChAT double-labeled cells. Thus, as previously demonstrated [12], we transfected LDTg cholinergic as well as non-cholinergic LDTg neurons and the transfected non-cholinergic neurons are likely to be either glutamatergic or GABAergic [28]. While cholinergic neurons are by definition confined to the LDTg, glutamatergic [28, 29] and GABAergic neurons [28] are found within the LDTg and in surrounding areas as well. In our studies, some eYFP expression was observed immediately outside the boundaries of the LDTg. The current angled virus injection approach aimed to avoid diffusion of virus into the ventricles immediately dorsal to the LDTg and to achieve uniform expression throughout the rostro-caudal extent of the LDTg. However, because the LDTg varies in both its dorso-ventral and medial-lateral extent at different rostro-caudal levels, restricting equal volumes of injected virus solution within LDTg boundaries at different rostro-caudal levels is difficult. Importantly, no eYFP expression was observed in surrounding areas that are known to send projections to the VTA and that participate in reward function, specifically the dorsal

raphe [30] and the pedunculopontine tegmental nucleus [13, 31]. VTA light stimulation, self-administered by rats during ICSS testing, is thus expected to have resulted in excitation of LDTg cholinergic, glutamatergic, and GABAergic inputs to the VTA. We show that the net effect of optogenetically driving LDTg inputs to the VTA during ICSS resulted in an increase in NAcc core DA overflow. For these reasons, excitation of VTA DA neurons by optogenetic excitation of LDTg inputs is likely mediated by cholinergic and glutamatergic receptor mechanisms in the VTA, as has been previously shown for the increases in NAcc core DA release induced by electrical stimulation of LDTg cell bodies in anesthetized rats [17]. In mice, selective VTA optogenetic excitation of either LDTg-glutamatergic or LDTg-cholinergic inputs to the VTA each result in rewarding effects in an operant place preference paradigm [14]. Similarly in rats, selective VTA optogenetic excitation of LDTg-cholinergic inputs during confinement to one chamber of a conditioned place preference apparatus, results in acquisition of Pavlovian conditioned place preference [13]. Future studies in which ChR2 is selectively targeted to LDTg-cholinergic or glutamatergic cell populations in the rat will clarify their contributions to exciting mesolimbic DA signaling in the ICSS paradigm. However, while ChAT::Cre rats are available in this regard (see for example [13, 32, 33]), these studies will have to await the availability of VGluT2::Cre rats.

Consistent with a report that the LDTg provides some input to the substantia nigra pars compacta (SNc; 13), we observed some eYFP expression lateral to the VTA in parts of the SNc. Infusions of cholinergic agonists into the SNc increase striatal DA efflux in anesthetized rats [34] and selective optogenetic excitation of SNc DA cells reinforces operant responding in mice [35]. However, targeted optogenetic excitation of LDTg terminals in SNc does not support the acquisition of Pavlovian conditioned place preference in rats [13]. Thus it seems unlikely that concurrent excitation of LDTg inputs to the SNc significantly contributed to the observed reinforcing effects of VTA stimulation in the current studies.

Blockade of either D1 or D2 DA receptors in the core and shell of the NAcc reduced the total amount of lever-pressing for optogenetic excitation of LDTg inputs to the VTA, a finding consistent with the effects of D1 and D2 DA receptor antagonists on stimulant-induced behavioral activation [36, 37] and their targeting of D1 and D2 dopamine receptor expressing spiny projection neurons in the NAcc [38–40]. The pattern of operant responding observed following pre-treatment with SCH23390 or raclopride, D1 and D2 dopamine receptor antagonists respectively, was similar. In either case, rats initiated responding with normal latencies when testing sessions began and the response levers became available. Rats lever-pressed in each case at rates comparable to those observed under conditions of saline pre-treatment for the first 6–11 minutes of the session followed by significant reductions in reinforced lever pressing rates. Similar patterns of responding were previously observed following systemic pre-treatment with the broad-spectrum DA receptor antagonist flupenthixol [12] and, are reminiscent of the extinction-like effects of systemic DA receptor blockade on responding for rewarding electrical brain stimulation in rats [41]. As the antagonists were given locally in the current studies, leading to fast receptor blockade, the pattern of responding suggests that rats reduced lever-pressing rates only after they experienced VTA optical stimulation under conditions of DA receptor blockade (i.e. after the first 6–11 minutes of the session, depending on the antagonist used). Importantly, infusions

into the NAcc of SCH23390 or raclopride at doses similar to or higher than those used here do not affect locomotor activity [23–25], free food consumption, or lever pressing under a fixed ratio-1 schedule [42]. Thus, the present results taken together indicate that DA released into the NAcc core contributes critically to the reinforcing effects of optogenetic ICSS of LDTg inputs to the VTA by acting at D1 and D2 DA receptors in this site. This is consistent with previous findings in anesthetized rats showing that electrical stimulation of LDTg cell bodies increases DA efflux in the NAcc core as measured by in vivo chronoamperometry [17].

Our results add to a number of previous reports that support an important role of mesopontine inputs (LDTg or PPTg) to the VTA in reward [12–15, 31, 33] but also point to some inconsistencies. Of most relevance here is a previous study in mouse which used an elegant combination of anatomical and electrophysiological techniques to show that LDTg inputs activate predominantly (though not exclusively; present results) DA neurons in the lateral VTA that project to the lateral portions of the NAcc shell [15]. Selective unilateral optogenetic activation of these VTA-projecting LDTg cell bodies, during confinement to one chamber of a conditioned place preference apparatus, resulted in acquisition of Pavlovian conditioned place preference. Furthermore, combined SCH 23390/raclopride pre-treatment in the lateral portions of the NAcc shell, administered ipsilaterally to optical VTA stimulation, prevented the acquisition of Pavlovian conditioned place preference. Our results contrast with these findings as we show that (1) driving LDTg inputs to the VTA increases DA overflow in the NAcc core, and (2) activation of D1 and D2 DA receptors in this site is necessary for the reinforcing effects of optogenetic ICSS of LDTg inputs to the VTA. Because of the findings of Lammel et al. [15] in the lateral NAcc shell, we also assessed the effect of D1 and D2 DA receptor blockade in the medial NAcc shell and found these receptors to be critical as well. Thus, DA receptor activation in both core and shell NAcc subnuclei appears critical for the reinforcing effects of optogenetic ICSS of LDTg inputs to the VTA. Although, effects on DA overflow in the NAcc shell subregions remain to be assessed.

Possible differences between the circuitry under investigation in the rat and mouse brain are worth considering here. In rats, LDTg injections of an anterograde tracer [16] or fluorescent viral opsin transfection of LDTg cholinergic neurons [33] each result in uniform labeling of axons throughout the VTA. Consistent with this we found uniform eYFP expression throughout the VTA following viral transfection of LDTg neurons. Fluorogold injections into the NAcc that impinge on both core and medial shell regions result in retrograde labeling of VTA projection neurons many of which receive excitatory LDTg inputs [16]. The boundaries between the lateral and medial NAcc shell have not been clearly defined. In the rat brain, the lateral shell appears to lie between Bregma AP +0.84 and +2.16 [20]. It is worth noting that our histological analysis revealed dialysis probe and injection cannulae placements that were for the most part rostral to Bregma +2.16. The extent to which the LDTg projects to VTA DA neurons that give rise to NAcc lateral shell projections in the rat brain has not been systematically investigated. However, electrophysiological evidence in rats indicates that excitation of LDTg-cholinergic terminals in the VTA excites VTA DA cells that have been retrogradely labeled by tracer injections into the lateral shell of the NAcc [33] and this subnucleus clearly contributes to the expression of motivated behaviors

[43, 44]. Our results do not rule out a contribution of dopaminergic projections to this site in the reinforcing effects elicited by excitation of LDTg inputs to the VTA. We neither sampled DA overflow nor tested the effects of D1/D2 DA receptor antagonists in the lateral shell of the NAcc. Our findings are, however, consistent with existing anatomical findings in rats showing that DA receptor blockade in either NAcc core or medial shell effectively reduces the reinforcing effects mediated by LDTg inputs to the VTA. Our findings are also consistent with a previous report in anesthetized mice showing increases in NAcc core DA efflux induced by electrical stimulation of LDTg cell bodies [45].

The non-contingent optogenetic excitation used in conditioned place preference studies and the contingent optogenetic self-stimulation used in the current studies also differ in obvious ways. There is general consensus that conditioned place preference reflects seeking of/preference for the stimulus properties of an environment which have acquired incentive value through classical conditioning [46, 47]. Self-administration on the other hand, where the probability of a behavior increases as a result of the experimental contingency, is generally thought to measure reinforcement. Many commonalties exist between findings obtained using the two paradigms. Most drugs of abuse that are self-administered by rats also lead to the acquisition of conditioned place preference (for a comprehensive review see [47]). However, the neural mechanisms that underlie drug self-administration and the acquisition of conditioned place preference do not appear to be identical. For example, NAcc (core or shell) D2 DA receptor blockade prior to daily cocaine conditioning sessions does not disrupt the acquisition of conditioned place preference [48], while NAcc core D2 DA receptor blockade reduces cocaine reinforcement in an intravenous self-administration paradigm [21]. Whether different neural pathways and mechanisms are recruited by experimental paradigms in which optogenetic excitation of brain circuits is (e.g. ICSS) or is not contingent (e.g. conditioned place preference) on responding has not been systematically investigated.

In conclusion, the present data are consistent with previous studies showing that the LDTg regulates mesolimbic DA signaling in anesthetized animal preparations [9, 17, 33, 45] and that exciting LDTg inputs to the VTA is reinforcing and rewarding [12–15]. Our results demonstrate that projections from the VTA to the NAcc core and medial shell each critically contribute, via their action on D1 and on D2 DA receptors, to the reinforcing effects of increasing excitatory LDTg drive to the VTA.

## Acknowledgments

We thank Dr. Karl Deisseroth for making the AAV-CaMKIIα-ChR2(H134R)-eYFP and AAV-CamKIIα-eYFP viral vector constructs available to us. This work was funded by start-up funds provided to SS by Loyola University Chicago, a Loyola University Mulcahy Undergraduate Fellowship to DP, and US National Institutes of Health grants R15 DA041694 to SS and R01 DA09397 to PV.

## References

1. Bromberg-Martin ES, Matsumoto M, Hikosaka O. Dopamine in motivational control: rewarding, aversive, and alerting. Neuron. 2010; 68:815–834. [PubMed: 21144997]

2. Di Chiara GG, Imperato A. Drugs abused by humans preferentially increase synaptic dopamine concentrations in the mesolimbic system of freely moving rats. Proc Natl Acad Sci USA. 1988; 85:5274–5278. [PubMed: 2899326]

3. Schultz W, Apicella P, Ljungberg T. Responses of monkey dopamine neurons to reward and conditioned stimuli during successive steps of learning a delayed response task. J Neurosci. 1993; 13:900–913. [PubMed: 8441015]

4. Schultz W. Multiple dopamine functions at different time courses. Annu Rev Neurosci. 2007; 30:259–288. [PubMed: 17600522]

5. Wise RA. Forebrain substrates of reward and motivation. J Comp Neurol. 2005; 493:115–121. [PubMed: 16254990]

6. Watabe-Uchida M, Zhu L, Ogawa SK, Vamanaro A, Uchida NN. Whole-brain mapping of direct inputs to midbrain dopamine neurons. Neuron. 2012; 74:858–873. [PubMed: 22681690]

7. Geisler S, Zahm DS. Afferents of the ventral tegmental area in the rat – anatomical substratum for integrative functions. J Comp Neurol. 2005; 490:270–294. [PubMed: 16082674]

8. Floresco S, West AR, Ash B, Moore H, Grace AA. Afferent modulation of dopamine neuron firing differentially regulates tonic and phasic dopamine transmission. Nat Neurosci. 2003; 6:968–73. [PubMed: 12897785]

9. Lodge DJ, Grace AA. The laterodorsal tegmentum is essential for burst firing of ventral tegmental area dopamine neurons. Proc Natl Acad Sci USA. 2006; 103:5167–5172. [PubMed: 16549786]

10. Oakman SA, Faris PL, Kerr PE, Cozzari C, Hartman BK. Distribution of pontomesencephalic cholinergic neurons projecting to substantia nigra differs significantly from those projecting to ventral tegmental area. J Neurosci. 1995; 15:5859–5869. [PubMed: 7666171]

11. Woolf NJ, Butcher LL. Cholinergic systems in the rat brain: III. Projections from the pontomesencephalic tegmentum to the thalamus, tectum, basal ganglia and basal forebrain. Brain Res Bull. 1986; 16:603–637. [PubMed: 3742247]

12. Steidl S, Veverka K. Optogenetic excitation of LDTg axons in the VTA reinforces operant responding in rats. Brain Res. 2015; 1614:86–93. [PubMed: 25911581]

13. Xiao C, Cho JR, Zhou C, Treweek JB, Chan K, McKinney SL, Yang B, Gradinaru V. Cholinergic Mesopontine Signals Govern Locomotion and Reward through Dissociable Midbrain Pathways. Neuron. 2016; 90:333–347. [PubMed: 27100197]

14. Steidl S, Wang H, Ordonez M, Zhang S, Morales M. Optogenetic excitation in the ventral tegmental area of glutamatergic or cholinergic inputs from the laterodorsal tegmental area drives reward. Eur J Neurosci. 2017; 45:559–571. [PubMed: 27740714]

15. Lammel S, Lim BK, Ran C, Huang KW, Betley MJ, Tye KM, Deisseroth K, Malenka RC. Input-specific control of reward and aversion in the ventral tegmental area. Nature. 2012; 491:212–217. [PubMed: 23064228]

16. Omelchenko N, Sesack SR. Laterodorsal tegmental projections to identified cell populations in the rat ventral tegmental area. J Comp Neurol. 2005; 483:217–235. [PubMed: 15678476]

17. Forster GL, Blaha CD. Laterodorsal tegmental stimulation elicits dopamine efflux in the rat nucleus accumbens by activation of acetylcholine and glutamate receptors in the ventral tegmental area. Eur J Neurosci. 2000; 23:3596–3604.

18. Bassareo V, De Luca MA, Di Chiara G. Differential impact of Pavlovian drug conditioned stimuli on in vivo dopamine transmission in the rat accumbens shell and core and in the prefrontal cortex. Psychopharmacology. 2007; 191:689–703. [PubMed: 17072592]

19. Everitt BJ, Robbins TW. Neural systems of reinforcement for drug addiction: from actions to habits to compulsion. Nat Neurosci. 2005; 8:1481–1489. [PubMed: 16251991]

20. Paxinos, G., Watson, C. The Rat Brain in Stereotaxic Coordinates. Elsevier Academic Press; San Diego: 2007.

21. Suto N, Ecke LERA. Wise Control of within-binge cocaine-seeking by dopamine and glutamate in the core of nucleus accumbens. Psychopharmacology. 2009; 205:431–439. [PubMed: 19436996]

22. Wise RA, Hoffman DC. Localization of drug reward mechanisms by intracranial injections. Synapse. 1992; 10:247–263. [PubMed: 1557697]

23. Neisewander JL, O'Dell LE, Redmond JC. Localization of dopamine receptor subtypes occupied by intra-accumbens antagonists that reverse cocaine-induced locomotion. Brain Res. 1995; 671:201–212. [PubMed: 7743209]
24. Hauber W, Münkle M. Motor depressant effects mediated by dopamine D2 and adenosine A2A receptors in the nucleus accumbens and the caudate-putamen. Eur J Pharmacol. 1997; 323:127–131. [PubMed: 9128830]
25. Van den Boss R, Cools AR, Ögren SO. Differential effects of the selective D2-antagonist raclopride in the nucleus accumbens of the rat on spontaneous and *d*-amphetamine-induced activity. Psychopharmacology. 1988; 95:447–451. [PubMed: 2975012]
26. Mesulam MM, Mufson EJ, Wainer BH, Levey AI. Central cholinergic pathways in the rat: an overview based on an alternative nomenclature (Ch1–Ch6). Neuroscience. 1983; 10:1185–1201. [PubMed: 6320048]
27. Woolf NJ. Cholinergic systems in mammalian brain and spinal cord. Prog Neurobiol. 1991; 37:475–524. [PubMed: 1763188]
28. Wang HL, Morales M. Pedunculopontine and laterodorsal tegmental nuclei contain distinct populations of cholinergic, glutamatergic and GABAergic neurons in rats. Eur J Neurosci. 2009; 29:340–358. [PubMed: 19200238]
29. Geisler S, Derst C, Veh RW, Zahm D. Glutamatergic afferents of the ventral tegmental area in the rat. J Neurosci. 2007; 27:5730–5743. [PubMed: 17522317]
30. Qi J, Zhang S, Wang HL, Wang H, de Jesus Aceves Buendia J, Hoffman AF, Lupica CR, Seal RP, Morales M. A glutamatergic reward input from the dorsal raphe to ventral tegmental area dopamine neurons. Nat Commun. 2014; 5:5390. [PubMed: 25388237]
31. Yeomans JS, Mathur A, Tampakeras M. Rewarding brain stimulation: role of tegmental cholinergic neurons that activate dopamine neurons. Behav Neurosci. 1993; 107:1077–1087. [PubMed: 8136061]
32. Witten IB, Steinberg EE, Lee SY, Davidson TJ, Zalocusky KA, Brodsky M, Yizhar O, Cho SL, Gong S, Ramakrishnan C, Stuber GD, Tye KM, Janak PH, Deisseroth K. Recombinase-driver rat lines: tools, techniques, and optogenetic application to dopamine-mediated reinforcement. Neuron. 2011; 72:721–733. [PubMed: 22153370]
33. Dautan D, Souza AS, Huerta-Ocampo I, Valencia M, Assous M, Witten IB, Deisseroth K, Tepper JM, Bolam JP, Gerdjikov TV, Mena-Segovia JJ. Segregated cholinergic transmission modulates dopamine neurons integrated in distinct functional circuits. Nat Neurosci. 2016; 19:1025–1033. [PubMed: 27348215]
34. Miller AD, Blaha CD. Midbrain muscarinic receptor mechanisms underlying regulation of mesoaccumbens and nigrostriatal dopaminergic transmission in the rat. Eur J Neurosci. 2005; 21:1837–1846. [PubMed: 15869479]
35. Ilango A, Kesner AJ, Keller KL, Stuber GD, Bonci A, Ikemoto S. Similar roles of substantia nigra and ventral tegmental dopamine neurons in reward and aversion. J Neurosci. 2014; 34:817–822. [PubMed: 24431440]
36. Vezina P. $D_1$ dopamine receptor activation is necessary for the induction of sensitization by amphetamine in the ventral tegmental area. J Neurosci. 1996; 16:2411–2420. [PubMed: 8601820]
37. Anderson SM, Pierce RC. Cocaine-induced alterations in dopamine receptor signaling: Implications for reinforcement and reinstatement. Pharmacol Ther. 2005; 106:389–403. [PubMed: 15922019]
38. Gerfen CR, Surmeier DJ. Modulation of striatal projection systems by dopamine. Ann Rev Neurosci. 2011; 34:441–466. [PubMed: 21469956]
39. Kupchik YM, Brown RM, Heinsbroek JA, Lobo MK, Schwartz DJ, Kalivas PW. Coding the direct/indirect pathways by D1 and D2 receptors is not valid for accumbens projections. Nature Neurosci. 2015; 18:1230–1232. [PubMed: 26214370]
40. Heinsbroek JA, Neuhofer DN, Griffin WC III, Siegel GS, Bobadilla A-C, Kupchik YM, Kalivas PW. Loss of plasticity in the D2-Accumbens pallidal pathway promotes cocaine seeking. J Neurosci. 2017; 37:757–767. [PubMed: 28123013]

41. Fouriezos G, Wise RA. Pimozide-induced extinction of intracranial self- stimulation: response patterns rule out motor or performance deficits. Brain Res. 1976; 103:377–380. [PubMed: 1252926]
42. Yun IA, Nicola SM, Fields HL. Contrasting effects of dopamine and glutamate receptor antagonist injection in the nucleus accumbens suggest a neural mechanism underlying cue-evoked goal-directed behavior. Eur J Neurosci. 2004; 20:249–263. [PubMed: 15245497]
43. Bossert JM, Poles GC, Wihbey KA, Koya E, Shaham Y. Differential effects of blockade of dopamine D1-family receptors in nucleus accumbens core or shell on reinstatement of heroin seeking induced by contextual and discrete cues. J Neurosci. 2007; 27:12655–12663. [PubMed: 18003845]
44. Ikemoto S. Dopamine reward circuitry: two projection systems from the ventral midbrain to the nucleus accumbens-olfactory tubercle complex. Brain Res Rev. 2007; 56:27–78. [PubMed: 17574681]
45. Forster GL, Yeomans JS, Takeuchi J, Blaha CD. M5 muscarinic receptors are required for prolonged accumbal dopamine release after electrical stimulation of the pons in mice. J Neurosci. 2002; 22:RC190. [PubMed: 11756520]
46. Huston JP, Silva MA, Topic B, Müller CP. What's conditioned in conditioned place preference? Trends Pharmacol Sci. 2013; 34:162–166. [PubMed: 23384389]
47. Bardo MT, Bevins RA. Conditioned place preference: what does it add to our preclinical understanding of drug reward? Psychopharmacology. 2000; 153:31–43. [PubMed: 11255927]
48. Baker DA, Khroyan TV, O'Dell LE, Fuchs RA, Neisewander JL. Differential effects of intra-accumbens sulpiride on cocaine-induced locomotion and conditioned place preference. J Pharmacol Exp Ther. 1996; 279:392–401. [PubMed: 8859018]

## Highlights

- Rats acquire VTA optogenetic intracranial self-stimulation (ICSS) of LDTg inputs
- This ICSS increases DA overflow in the forebrain NAcc
- D1 or D2 receptor blockade in the NAcc reduces optogenetic ICSS of LDTg inputs to the VTA

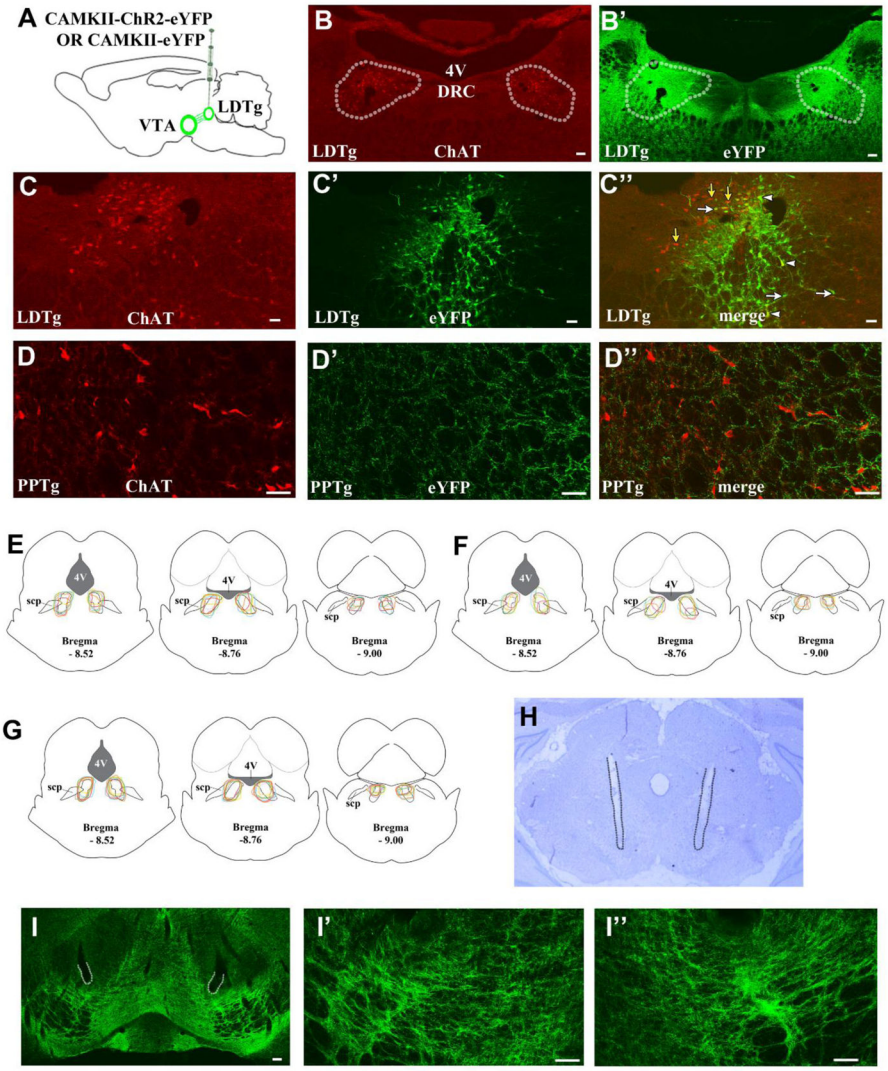


31

**Figure 1. LDTg transfection with AAV5-CAMKII-ChR2-eYFP results in eYFP expression within the LDTg and the VTA**

**A.** LDTg neurons were bilaterally transfected with AAV5-CAMKII-ChR2-eYFP or AAV5-CAMKII-eYFP in rats. **B–B′.** The boundaries of the LDTg are defined by the extent of ChAT labeling (traced according to B) and are superimposed on to the image in B′. Bilateral eYFP expression was observed within the boundaries of the LDTg (B′). **C–C″.** eYFP-labeled (white arrows), eYFP/ChAT double-labeled (white arrow heads) and ChAT single-labeled (yellow arrows) cells were observed within the LDTg. **D–D″.** No eYFP-labeled cells (D′) were observed within the adjacent PPTg, located rostral and lateral to the LDTg (defined by ChAT expression; D). However, eYFP-labeled processes were observed within

the proximity of ChAT-labeled cells (D″). **E–G.** Schematic representations of eYFP expression in relation to LDTg boundaries (dashed outlines) in rats transfected with AAV5-CAMKII-ChR2-eYFP used for the NAcc microdialysis studies (E; n = 6), the NAcc core D1/D2 DA receptor antagonist studies (F; n = 6), or the NAcc shell D1/D2 DA receptor antagonist studies (G; n = 7). Outlines for individual rats are shown in different colors at three A-P levels. eYFP expression was consistently observed within the boundaries of the LDTg. **H.** Representative cresyl-violet stained section showing the VTA and bilateral optic probes (tracks marked by dotted lines). VTA fiber optic tip placements for individual rats are shown in Fig 2B. **I–I″.** eYFP expression was observed in the VTA following LDTg transfection with AAV5-CAMKII-ChR2-eYFP. The areas adjacent to probe tips outlined at low magnification in I are shown at higher magnification in I′ (left VTA) and I″ (right VTA). Scale bars: 100 μm in B, B′, I; 50 μm in C, C′, C″, D, D′, D″, I′, I″. DRC, dorsal raphe nucleus, caudal part. scp, superior cerebellar peduncle. 4V, 4$^{th}$ ventricle.

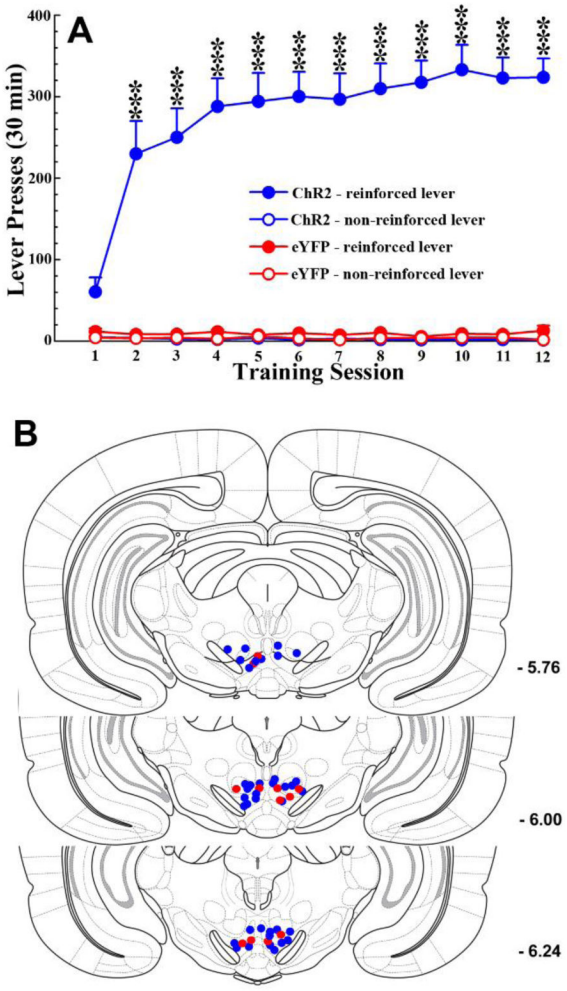


**Figure 2. Optogenetic excitation of LDTg inputs to the VTA reinforces lever-pressing in rats**

**A.** ChR2 (n = 19; blue lines), but not eYFP (n = 6; red lines), rats acquired intracranial self-stimulation to excite LDTg inputs to the VTA. ChR2 rats pressed the reinforced lever (filled circles) significantly more than the non-reinforced lever (open circles) in each of the 2$^{nd}$ through 12$^{th}$ training sessions (*** $p < 0.001$). eYFP rats pressed either lever at very low numbers. Each press on the reinforced lever resulted in a 1.5 s train of 10ms light pulses at 20Hz. **B.** Bilateral VTA placements of optic fiber tips in ChR2 (n = 19; blue circles) and eYFP (n = 6; red circles) rats. These rats were subsequently used in the NAcc microdialysis and DA receptor antagonist studies.

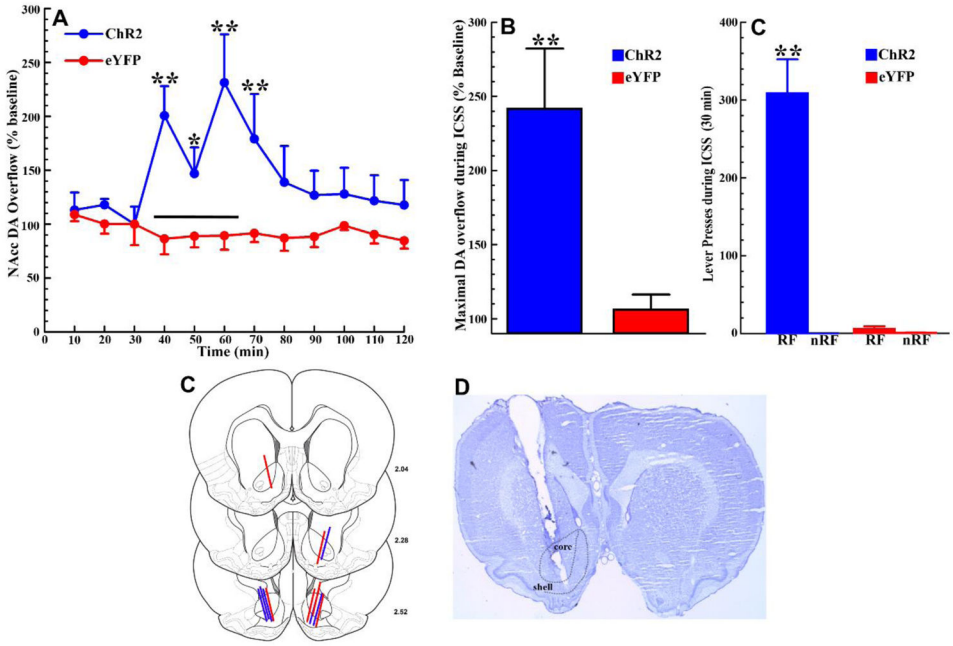


**Figure 3. Optogenetic ICSS of LDTg inputs to the VTA increases NAcc DA overflow**

**A.** Time course of NAcc DA overflow before (10–30 min), during (40–60 min), and after (70–120 min) a 30-min ICSS session (black bar). Samples were collected every ten minutes and are expressed as a percentage of baseline levels. In ChR2 rats (blue line), NAcc DA overflow increased during the ICSS session, when rats were lever-pressing to excite LDTg inputs to the VTA (C), and returned to baseline levels over the course of the hour following termination of the ICSS session. In eYFP rats (red lines), which did not lever-press during the ICSS session (C), NAcc DA overflow fluctuated around baseline levels throughout the sampling period (* $p < 0.05$, ** $p<0.01$; comparing ChR2 to eYFP rats for a time bin). **B.** Maximal NAcc DA overflow increased during optogenetic VTA excitation of LDTg inputs to approximately 240% of baseline levels in ChR2 rats (n = 6; blue bar). In eYFP rats (n = 6; red bar) maximal NAcc DA overflow did not increase significantly above baseline levels during the ICSS period (** $p<0.01$). **C.** During the NAcc microdialysis session, as during the ICSS training period (Fig 2A), ChR2 rats (n= 6; blue bars) pressed the reinforced lever (RF) significantly more than the non-reinforced lever (nRF) and significantly more than eYFP rats pressed the reinforced lever (** $p<0.01$). eYFP rats (n = 6; red bars) pressed either lever at very low levels. The total numbers of presses on the reinforced lever in ChR2 rats was slightly lower during the microdialysis testing session than on the final training day but the difference was not statistically significant ($t_5 = 1.26$, $p>0.1$). **D.** NAcc dialysis probe placements in ChR2 (n = 6; blue lines) and eYFP rats (n=6; red lines). **E.** Representative cresyl-violet stained section showing a probe placement within the NAcc. All error bars show ± SEM.

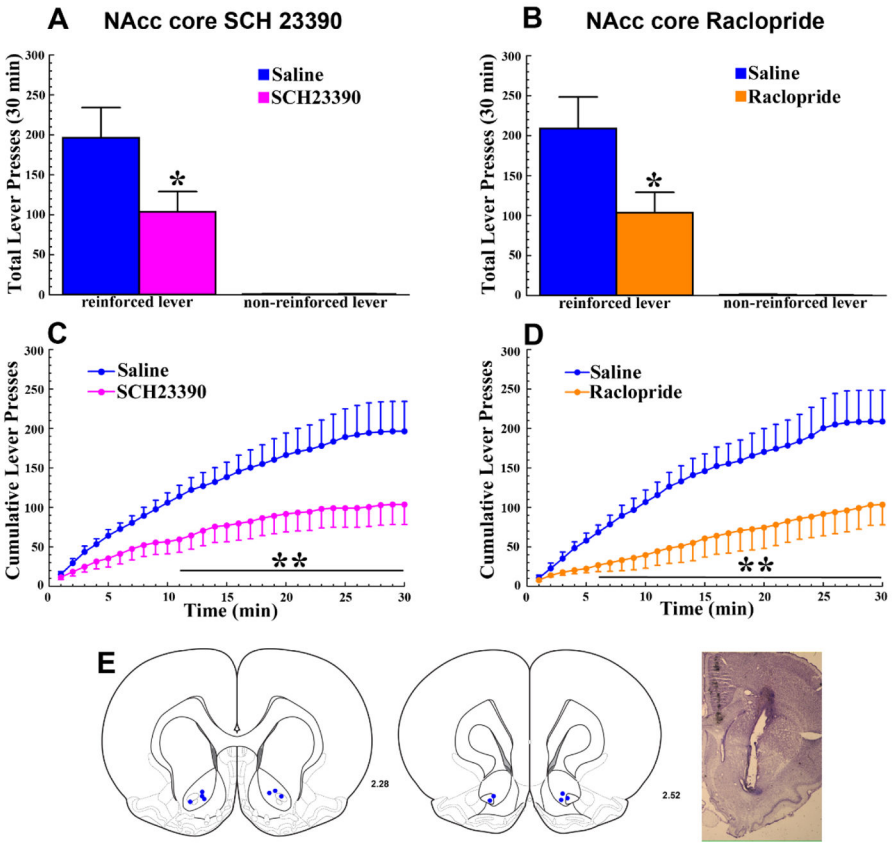


**Figure 4. The reinforcing effects of optogenetic ICSS of LDTg inputs to the VTA require the activation of D1 and D2 DA receptors in the NAcc core**

**A and B.** Relative to saline, bilateral infusion of either the D1-selective antagonist SCH 23390 (A; 0.6μg/0.3μl, pink bar) or the D2-selective antagonist Raclopride (B; 1μg/0.3μl, orange bar) into the NAcc core reduced the total numbers of lever presses on the reinforced, but not on the non-reinforced, lever (* $p < 0.05$). **C and D**. Time course analyses of cumulative reinforced lever presses following the bilateral NAcc core SCH-23390 (C) or Raclopride (D) infusions show a gradual manifestation of the receptor antagonist effects. Relative to saline (blue lines), reinforced lever pressing was significantly reduced from 11–30 (C; SCH23390) and 6–30 minutes (D; Raclopride) of the test session (p's<0.05–0.01) **E**. Left. Bilateral NAcc core injection sites for the 6 ChR2 rats tested (blue dots). **E**. Right. Representative cresyl violet-stained section showing a NAcc core injection site. All error bars show ± SEM.

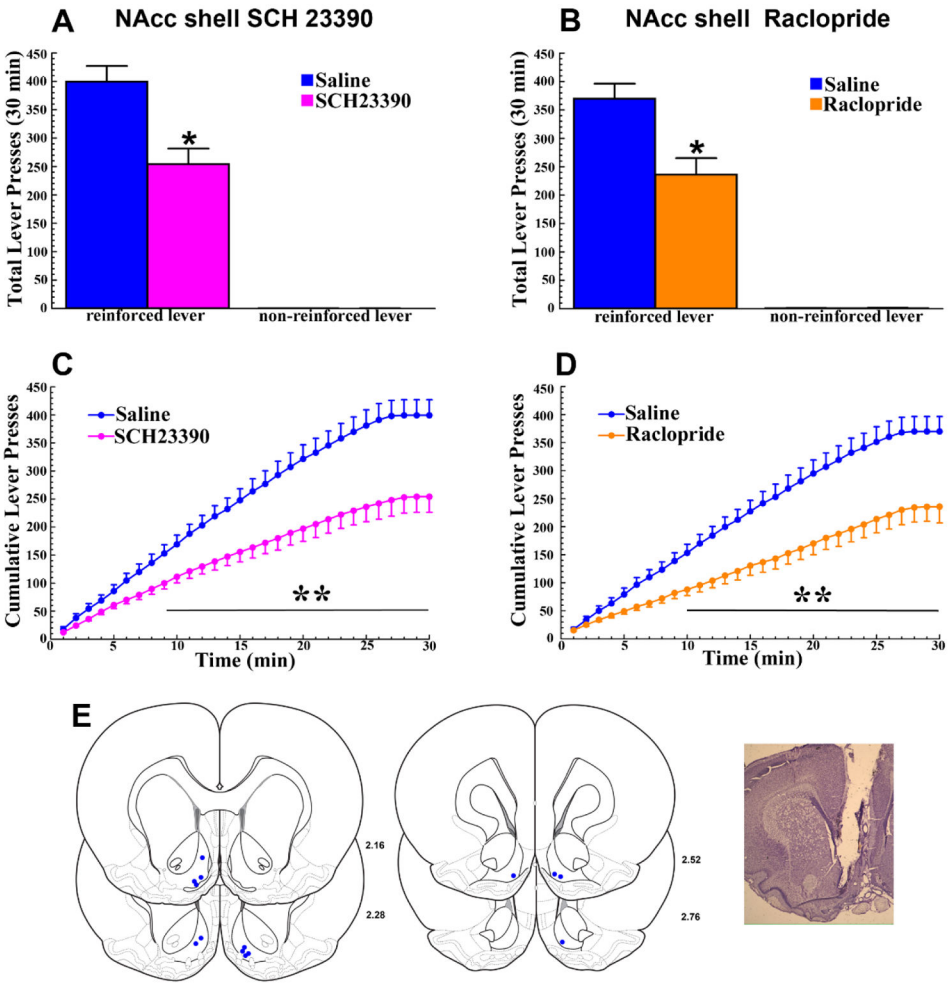


**Figure 5. The reinforcing effects of optogenetic ICSS of LDTg inputs to the VTA require the activation of D1 and D2 DA receptors in the NAcc shell**

Results are illustrated as described in Figure 4. Relative to saline (blue lines), reinforced lever pressing was significantly reduced from 9–30 (C; SCH23390) and 10–30 minutes (D; Raclopride) of the test session (p's<0.05–0.01). **E**. Left. Bilateral NAcc shell injection sites for the 7 ChR2 rats tested (blue dots). **E**. Right. Representative cresyl violet-stained section showing a NAcc shell injection site.

**Table 1**

Different groups and final numbers of rats used for data analysis in the NAcc microdialysis and DA receptor antagonist microinjection studies

| LDTg Transfection | Group | n/group |
|---|---|---|
| ChR2 | NAcc μdialysis | 6 |
| | NAcc core DAR antagonists | 6 |
| | NAcc shell DAR antagonists | 7 |
| eYFP | NAcc μdialysis | 6 |

Note: Of the original 33 rats prepared, 6 ChR2 and 2 eYFP rats were dropped either because eYFP was detected outside the LDTg (6) or because cannula placements were found outside the NAcc (2).